Carbohydrate Polymers 74 (2008) 946–952

Contents lists available at ScienceDirect

Carbohydrate Polymers

journal homepage: www.elsevier.com/locate/carbpol

Structural characterization and properties of starch/konjac glucomannan blend films

Jianguang Chen [b], Changhua Liu [b], Yanqing Chen [b], Yun Chen [a,c], Peter R. Chang [a,*]

[a] Bioproducts and Bioprocesses National Science Program, Agriculture and Agri-Food Canada, 107 Science Place, Saskatoon, SK, Canada S7N 0X2
[b] College of Chemistry and Chemical Engineering, Southwest University, 400715 Chongqing, China
[c] Research Centre for Medical and Structural Biology, School of Basic Medical Science, Wuhan University, Wuhan 430071, China

ARTICLE INFO

Article history:
Received 25 April 2008
Received in revised form 26 May 2008
Accepted 27 May 2008
Available online 5 June 2008

Keywords:
Starch
Konjac glucomannan
Structure
Blend film

ABSTRACT

In this work, a series of glycerol-plasticized pea starch/konjac glucomannan (ST/KGM) blend films was prepared by a casting and solvent evaporation method. The structure, thermal behavior, and mechanical properties of the films were investigated by means of Fourier Transform Infrared Spectroscopy, wide-angle X-ray diffraction, scanning electron microscopy, differential scanning calorimetry, and tensile testing. The results indicated that strong hydrogen bonding formed between macromolecules of starch (ST) and konjac glucomannan (KGM), resulting in a good miscibility between ST and KGM in the blends. Compared with the neat ST, the tensile strength of the blend films were enhanced significantly from 7.4 to 68.1 MPa with an increase of KGM content from 0 to 70 wt%. The value of elongation at break of the blend films was higher than that of ST and reached a maximum value of 59.0% when the KGM content was 70 wt% and 20% of glycerol as plasticizer. The incorporation of KGM into the ST matrix also led to an increase of moisture uptake for the ST-based materials. The structure and properties of pea starch-based films were modified and improved by blending with KGM.

1. Introduction

Recently, biopolymers have received much attention in academia and industry due to the concerns of environmental threats, as well as the costs and supply of petroleum (Ishiaku, Pang, Lee, & Mohd, 2002; Jansson, Järnström, Rättö, & Thuvander, 2006; Ma & Yu, 2004; Nakamura, Cordi, Almeida, Duran, & Mei, 2005; Pracella, Pazzagli, & Galeski, 2002; Yu, Dean, & Li, 2006). Starch (ST) contains two macromolecules: amylose, which is essentially linear; and amylopectin, which is highly branched. Starch therefore has three free hydroxyl groups in each glycoside ring. As a renewable raw material with low cost, starch has shown promising applications in the fields of agriculture, industry, food engineering and medicine as biodegradable plastics (Huang & Yu, 2005), composites and films (Córdoba, Cuéllar, González, & Medina, 2008), edible films (Chillo et al., 2008), food hydrocolloids (Singh, Kaur, & McCarthy, 2007), surface coatings (Patil, Fanta, Felker, & Salch, 2008), packaging materials (Jagannath, Radhika, Nanjappa, Murali, & Bawa, 2006; Maurizio, Jan, & Vlieger, 2005) and drug delivers (Szepes et al., 2008). Unfortunately, ST-based composite materials have the disadvantage of poor mechanical properties, which severely limited their applications. Some reports indicate that it is difficult to obtain high performance of tensile strength and elongation at break simultaneously. Generally, there are two approaches to overcome these drawbacks. One approach is to blend starch with other polymers with desirable or complementary properties (Avérous, Fauconnier, Moro, & Fringant, 2000; Godbole, Gote, Latkar, & Chakrabarti, 2003; Martin & Avérous, 2001; Seidenstücker & Fritz, 1998; Walia, Lawton, & Shogren, 2002; Walia, Lawton, Shogren, & Felker, 2000; Wang, Yang, & Wang, 2004). Not surprisingly, the mechanical properties and water-resistance of these ST-based blends also depend on the content of the non-ST polymers. Another approach is to prepare starch derivatives by replacing the hydrophilic —OH groups in the ST with hydrophobic groups via reactions such as esterification (Aburto et al., 1999; Fang, Fowler, Tomkinson, & Hill, 2002a; Fang, Fowler, Tomkinson, & Hill, 2002b; Fringant, Rinaudo, Foray, & Bardet, 1998; Parandoosh & Hudson, 1993; Sagar & Merrill, 1995; Wesslén, 1998; Wolff, Olds, & Hilbert, 1951) and etherification (Wesslén & Wesslén, 2002). However, additional costs would be incurred inevitably for those chemical modifications.

Konjac glucomannan (KGM) is a high molecular weight, water-soluble and non-ionic (neutral) polysaccharide found in roots and tubers of the *Amorphophallus konjac* plant. It has D-mannose (M) and D-glucose (G) in M/G molar ratio of 1.5–1.6 by β-1, 4-glycosidic linkages with about 1 acetyl group in every 17–19 sugar units at C-6 position (Liu & Xiao, 2004). KGM has been used widely in processed food, ink and paint, and biomedical materials (Calverta, Tepperc, Kammounib, Anderson, & Kritchevsky, 2006; Chen, Liu, & Zhuo, 2005). ST and KGM are edible hydrocolloids with excellent

* Corresponding author. Tel.: +1 306 956 7637; fax: +1 306 956 7247.
E-mail address: changp@agr.gc.ca (P.R. Chang).

0144-8617/$ - see front matter Crown Copyright © 2008 Published by Elsevier Ltd. All rights reserved.
doi:10.1016/j.carbpol.2008.05.021

film-forming capabilities, and have been recognized individually for their great potential (Calverta et al., 2006; Chen et al., 2005; Huang & Yu, 2005; Jagannath et al., 2006; Maurizio et al., 2005). In Particular, they have been incorporated into some selected edible films and coatings. In general, these films show advantages in decreasing the gas permeation rather than retardation of water loss due to their hydrophilic nature (Cheng, Karim, Norziah, & Seow, 2002). In the case of vegetables, the polysaccharide-based coatings play an important positive role in delaying senescence, and extending shelf life (García, Martino, & Zaritzky, 1998a; García, Martino, & Zaritzky, 1998b; García, Martino, Zaritzky, & Plata, 2000; Krochta & De Mulder-Johnston, 1997).

Recently, KGM was reported to interact synergistically with individual carrageenan, xanthan, gellan, and corn starch (Yoshimura, Takaya, & Nishinari, 1998). However, publications on the preparation and applications of ST and KGM as biodegradable films are scarce. The objective of the present work was to prepare ST/KGM blend films with potential applications as edible films, food surface coatings and biodegradable food packaging materials, and to study the effect of KGM on the performance of ST-based films. The structure, thermal and mechanical properties of the ST/KGM blend films were studied by Fourier transform infrared spectroscopy (FT-IR), wide-angle X-ray diffraction (XRD), scanning electron microscope (SEM), thermogravimetric analysis (TG), differential scanning calorimetry (DSC), and tensile test. In addition, the relationship between the structure and properties of the ST/KGM films was also discussed.

2. Experimental method

2.1. Materials

Pea starch (ST), with average granule size of about 29 μm and composed of 35% amylose and 65% amylopectin, was supplied by Nutri-Pea Limited Canada (Portage la Prairie, Manitoba, Canada). Konjac glucomannan (KGM) was purchased from Shiyan Huaxianzi Konjac Productions Co., Ltd. (Shiyan, China). The plasticizer, glycerol (99% purity), was from Maoye Chemical Co. (Chongqing, China).

2.2. Film preparation

The glycerol-plasticized ST/KGM blend films were fabricated by means of a casting and solvent evaporation process (Mathew, Brahmakumar, & Emilia Abraham 2006). ST solutions (5 wt%) were prepared by dispersing 11 g of starch in 220 mL glycerol solution (the glycerol content is 0.75 wt%). The starch mixture aqueous suspension was stirred at 95 °C in water bath for 1h until the solution became transparent and the starch paste was obtained. KGM and glycerol were dispersed in distilled water and stirred at room temperature for 1 h. After the KGM was dissolved completely, the solutions were filtered with cheese cloth and the insoluble residue if any was filtered out leaving a concentration of 1 wt%. The KGM mixture therefore contained 1 wt% of KGM, 0.15 wt% of glycerol, and 98.85 wt% of water, respectively. Subsequently, ST/KGM mixture solutions were mixed and stirred for another 30 min. After degassing under vacuum, the composite was cast onto glass plates and then subjected to drying at 50 °C for 12 h to obtain dry films. By adjusting the KGM percent content in the solid compositions to 10, 30, 50, 70, and 90 wt%, respectively, a series of ST/KGM blend films with a thickness of around 0.1 mm were prepared and coded as s-k-g, where s and k is the percent content of ST and KGM in the solid compositions, respectively; and g is the percent content of glycerol in the plasticized film. For example, the film coded as 90-10-15 means that the percent content of ST and KGM in the solid compositions is 90 and 10 wt%, respectively, i.e. the original ratio of ST and KGM is 90:10; and the percent of glycerol in the film is 15 wt%, respectively. To serve as experimental controls, the neat ST films (s-k-g, s = 100, k = 0, and g = 10, 15, 20, respectively) and neat KGM films (s-k-g, s = 0, k = 100, and g = 10, 15, 20, respectively) were obtained using the same fabrication process. The codes for all films were listed in Table 1. Before various characterizations, the resulting films were kept in a conditioning desiccator of 43% relative humidity (RH) for more than one week at room temperature to ensure the equilibrium of the water in the films.

2.3. Fourier transform infrared spectroscopy

Fourier transform infrared spectroscopy (FT-IR) spectra of the blend films containing 15% glycerol in the mode of attenuated total reflection were recorded with a Nicolet (Madison, WI, USA) 170SX Fourier transform infrared spectrometer in the wavelength range of 4000–650 cm^{-1}.

2.4. X-ray diffractometry

X-ray diffraction (XRD) patterns of the samples were carried out with a XRD-3D, PuXi (Beijing, China) X-ray diffractometer under the following conditions: Nickel filtered Cu Kα radiation ($\lambda = 0.15406$ nm) at a voltage of 36 kV and current of 20 mA. The scanning rate was 4°/min in the angular range of 5–50° (2θ). To avoid the influence of relative humidity on relative crystallinity, ST/KGM blend films containing 15% glycerol were placed in desiccators and conditioned in the atmosphere of 43% *RH* for one week before XRD testing.

2.5. Scanning electron microscopy (SEM)

The films containing 15% glycerol were fractured in liquid nitrogen and the cross-sections were mounted on SEM stubs with double sided adhesive tape, and then coated with gold in a 13.3 Pa vacuum degree. Scanning electron microscope (S-4800, HITACHI, Japan) was taken to observe the morphologies of cross-sections for the samples at an accelerating voltage of 5 kV.

2.6. Thermal analyses

Thermal Gravimetric Analyses of ST/KGM blend films containing 15% glycerol was carried out on a TA-STDQ600 (TA Instruments Inc., New Castle, DE, USA). The thermo grams were acquired between 20 and 500 °C at a heating rate of 10 °C/min. Nitrogen was used as the purge gas at a flow rate of 20 mL/min. An empty pan was used as a reference. Differential Scanning Calorimetry (DSC) analyses of ST/KGM blend films containing 15% of glycerol were

Table 1
The code of ST/KGM blend films

KGM percent in KGM and ST (wt%)	0	10	30	50	70	90	100
10% glycerol	100-0-10	90-10-10	70-30-10	50-50-10	30-70-10	10-90-10	0-100-10
15% glycerol	100-0-15	90-10-15	70-30-15	50-50-15	30-70-15	10-90-15	0-100-15
20% glycerol	100-0-20	90-10-20	70-30-20	50-50-20	30-70-20	10-90-20	0-100-20

carried on a NETZSCH DSC 200 F3 (Netzsch Co, Selb/Bavaria, Germany). Nitrogen at a rate of 20 mL/min was used as the purge gas. Aluminum pans containing 2–3 mg of film were sealed using the DSC sample press. All samples were preheated with a scan rate of 20 °C/min over a temperature range of 25–100 °C and maintained at 100 °C for 10 min to remove the residual water, cooled to 25 °C, and heated up to 200 °C.

2.7. Mechanical properties

The tensile strength and elongation at break of the films were determined using a Micro-electronics Universal Testing Instrument Model Sans 6500 (Shenzhen Sans Test Machine Co. Ltd., Shenzhen, China) according to the Chinese standard method (GB 13022-91). The films were cut into 10 mm wide and 100 mm long strips and mounted between cardboard grips (150 × 300 mm) using adhesive so that the final area exposed was 10 × 50 mm. Before testing, the samples were kept at 43% *RH* for more than one week at room temperature to ensure the equilibration of the water in the films. The cross-head speed was 10 mm/min. All measurements were performed for three specimens and averaged.

2.8. Moisture uptake test

The moisture uptake of the ST/KGM blend films containing 15% glycerol was determined. The samples used were thin rectangular strips with dimension of 50 mm × 10 mm × 0.1 mm. They were vacuum-dried at 80 °C overnight and then kept for 0% *RH* (P_2O_5) for a week. After weighting, they were conditioned at room temperature in a desiccator of 98% *RH* ($CuSO_4{\cdot}5H_2O$ saturated solution) for one week to ensure the equilibrium of the moisture before testing. The moisture uptake (*MU*) of the samples was calculated as follows:

$$\mathrm{MU} = (W_1 - W_0)/W_0 \times 100\%$$

where W_0 and W_1 were the weight of the sample before exposure to 98% *RH* and after equilibrium, respectively. An average value of three replicates for each sample was taken.

3. Results and discussion

3.1. Fourier transform infrared spectroscopy

The FT-IR spectra of the films containing 15% glycerol are shown in Fig. 1. In the neat starch film (100-0-15), the stretching and bending vibration of the hydrogen bonding —OH groups of starch occurs at 3349 and 1641 cm^{-1}, respectively (Mathew et al., 2006). And the peaks at 869 and 1016 cm^{-1} are attributed to the C—O bond stretching in the ST. In the FT-IR spectrum of the neat KGM (0-100-15), the absorption peaks of hydrogen bonding hydroxyl groups of KGM, due to the complex stretch vibration associated with free inter- and intra-molecular bonding hydroxyl groups, occur at 3291 cm^{-1} and 1641 cm^{-1}, respectively (Krochta & De Mulder-Johnston, 1997). The absorption bands at 990 and 927 cm^{-1} are assigned to the stretching vibration of C—O.

In the typical spectrum of the ST/KGM composite films, the characteristic peaks of stretching vibration for both hydrogen-bonded hydroxyl and C—O groups show shifts with the variation of KGM content in the films. For example, the stretching vibrations of hydrogen-bonded hydroxyl groups locate at 3349 cm^{-1} in ST and 3291 cm^{-1} in KGM, respectively. But with an increase of KGM from 10% to 90%, this peak range from 3344 cm^{-1} (in the film 90-10-15) to 3311 (in the film 10-90-15). At the same time, the stretching vibration for both C—O locates at 1016 cm^{-1} in ST and at 990 cm^{-1} in KGM, respectively. However, this peak ranges from 1007 to 990 cm^{-1} with an increase of KGM from 10% to 90% in the composite films. All these changes indicate that strong hydrogen bonding interactions between KGM and ST in the composites has formed during the blending and film-forming process.

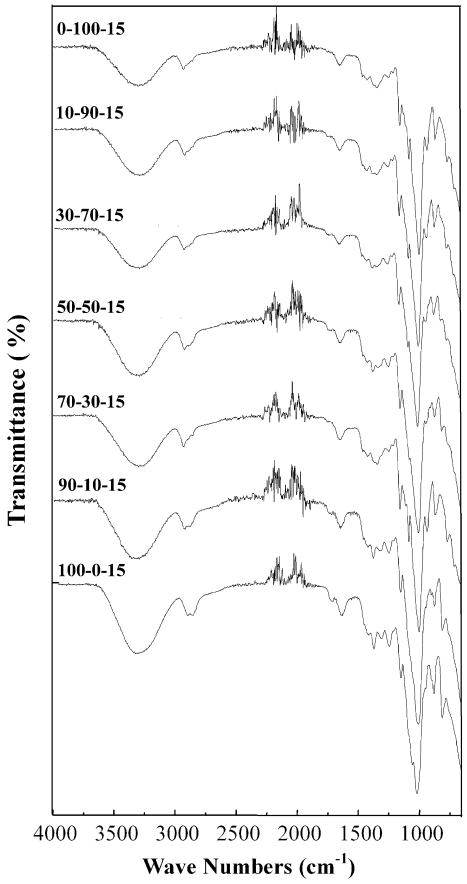

Fig. 1. FT-IR spectra of ST/KGM blend films with different KGM content.

3.2. X-ray diffractometry

The XRD patterns of the films containing 15% glycerol are shown in Fig. 2. The XRD patterns display a broad hump located around $2\theta = 18°$ with some low intensity diffraction peaks. For 100-0-15 film, the typical C-type crystallinity pattern with peaks at $2\theta = 5.7°$ (characteristic of B type polymorphs), 15.1° (characteristic of A type polymorphs), 17.21° (characteristic of both A and B type polymorphs), 20.18° and 22.58° (characteristic of B type polymorphs) was observed clearly (Yoshimura et al., 1998). The crystalline structure was ascribed to spontaneous recrystallization or retrogradation of starch molecules after melting or gelatinization, which is similar to that often detected in the starchy food and thermoplastic material (Rindlav, Stading, Hermansson, & Gatenholm 1998). The XRD patterns of the neat KGM film (0-100-15) displays a broad hump located around $2\theta = 18°$ with ill-defined diffraction peaks, which indicates that the neat KGM is in the amorphous phase.

The incorporation of KGM has an effect on the crystalline structure of the ST. The crystallization diffraction peaks of the all ST/KGM samples are more than that of ST (100-0-15). On the whole, the XRD patterns of the ST/KGM composites still retained characteristic peaks of starch when the KGM content is lower than 50% (w/w). The diffraction peaks at around 5.71°, 15.1°, 17.21°, 20.18°, and 22.58° (2θ) could be identified in this case. However, the diffraction peak ($2\theta = 22.8°$) shifts to a lower number as KGM content increased. It indicates that the incorporation of KGM into starch matrix increases the distance of starch chain, decreases inter-molecular force, and increases the movement of starch chain.

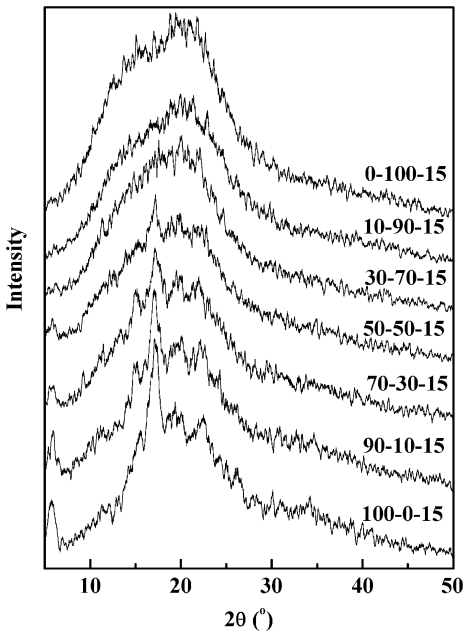

Fig. 2. XRD patterns of ST/KGM blend films.

Apparently, When KGM content increases ($\geqslant$50%), the broad hump located around $2\theta = 18^{\circ}$ displays ill-defined diffraction peaks. The samples 50-50-15, 30-70-15, and 90-10-15 are in the amorphous phase. This could be attributed to the amorphous KGM enwrapping ST, and decreasing the re-arrangement of starch molecular chains in the film-forming process.

3.3. Scanning electron microscopy (SEM)

The SEM photographs of the cross-sections for ST/KGM films (from 100-0-15 to 0-100-15) are shown in Fig. 3. The neat ST film (100-0-15) exhibits a rough cross-section due to the brittle properties fractured under liquid nitrogen circumstance, while the neat KGM film (0-100-15) exhibits relative smooth cross-sections because of its good film-forming properties and flexibility. With an increase of KGM content in the blend films, the cross-sections became more compact and less rough. When the KGM content is less than 50%, it dispersed as non-continuous phase in the ST matrix which is as continuous phase. However, the cross-section of 50-50-15 film exhibited different morphology from the other films. Some holes and small ditches can be observed on the cross-section of 50-50-15 film, indicating a certain degree of phase separation between ST and KGM. This is due to equivalent KGM and ST content in the film, which makes it difficult to identify which one is the continuous and which one is the non-continuous phase. Furthermore, when the KGM content is more than 50%, the cross-sections of the blend films became more smooth and compact. No obvious phase separation was observed in the cross-sections of 30-70-15 and 10-90-15 films. In those cases, ST would act as non-continuous phase in which it is dispersed well into a continuous KGM phase. Basically, due to the good compatibility of ST and KGM, no obvious phase separation was observed from SEM images when KGM content is lower than 30% or higher than 70%. In another word, the non-continuous phase, presumably from the lower

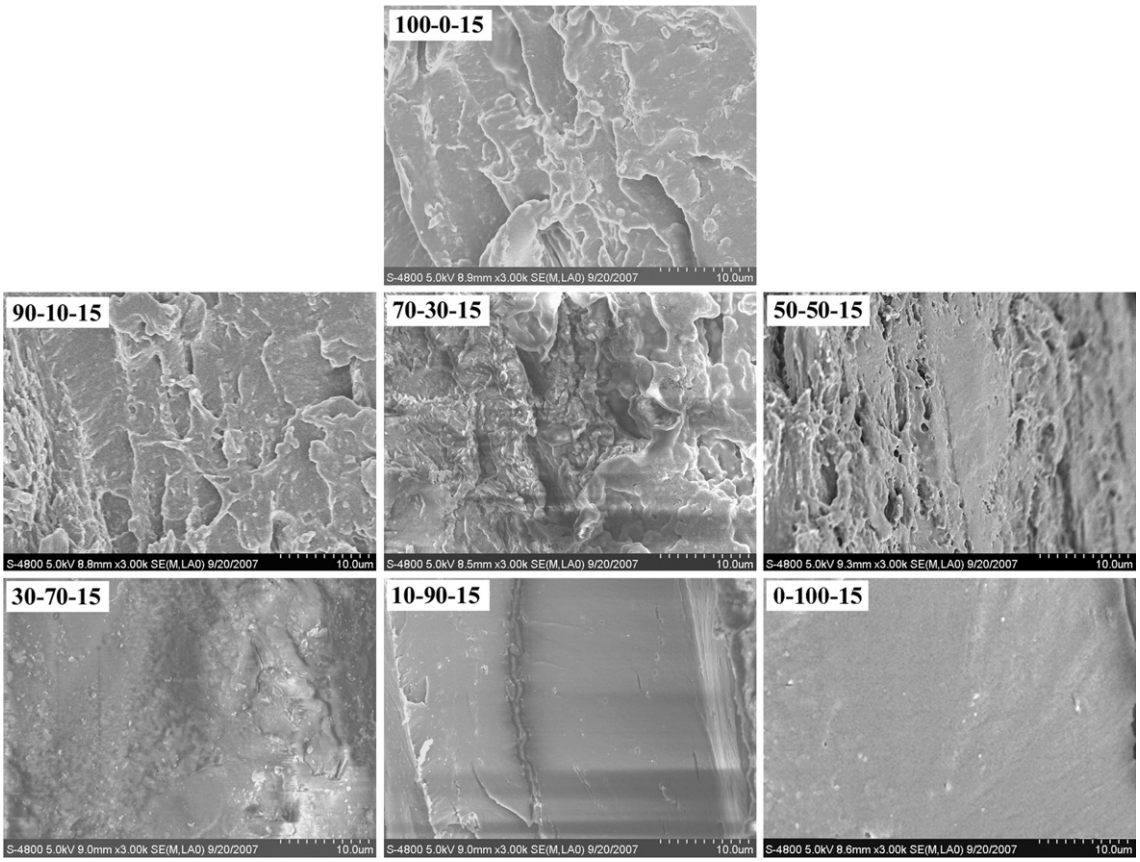

Fig. 3. SEM images of the failure surfaces for ST/KGM blend films.

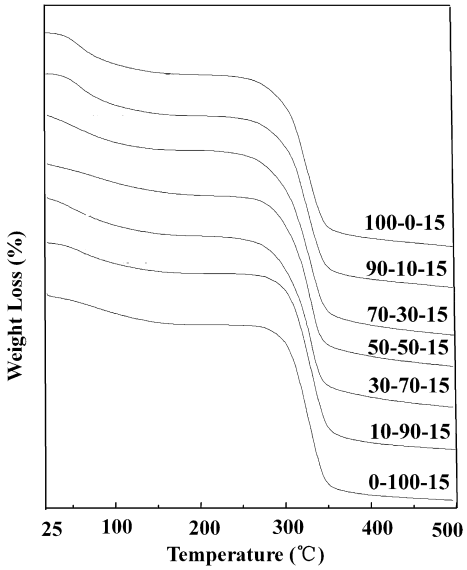

Fig. 4. TG curves of ST/KGM blend films with different KGM content.

content of KGM (or ST), can disperse relatively homogeneously in the continuous phase exerted by the high content of ST (or KGM).

3.4. Thermo gravimetric and differential scanning calorimetry analyses

The thermo gravimetric (TG) curves, shown in Fig. 4, are used to determine the weight loss of the material as it is heated. The initial weight loss of all samples at approximately 100 °C is due to the evaporation of water, while the weight loss in the second range (250–450 °C) corresponded to a complex process including the dehydration of the saccharide rings and depolymerization (Mathew & Dufresne, 2002). The TG curves show that all samples are stable up to 250 °C, with a maximum rate of decomposition occurring at 300 °C. Although the KGM content increased, the initial thermal decomposition temperature of the blend films is coincidental. This indicates that the thermo-stability of the starch-based films did not decrease with an increase of KGM content incorporated in the blend films.

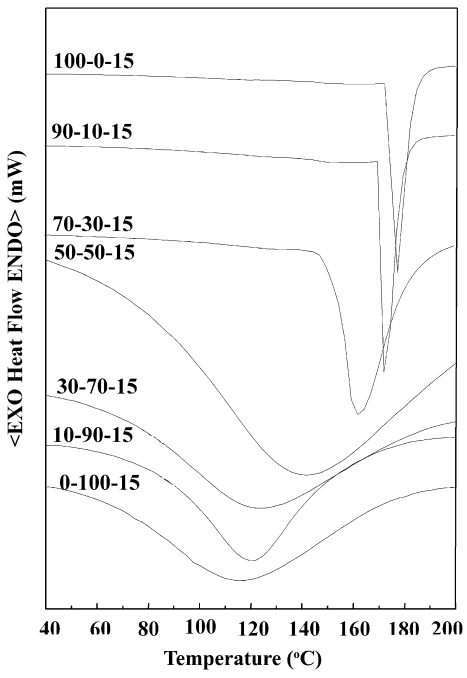

Fig. 5. DSC curves of ST/KGM blend films with different KGM content.

To further understand the structure and interaction between the two components, DSC studies of the ST/KGM blend films containing 15% glycerol are performed and shown in Fig. 5. Similar to the neat starch film containing 15% glycerol (100-0-15), an endothermic peak at about 180–115 °C in the composite films (from 90-10-15 to 10-90-15), attributed to the melting of ST/KGM crystallinity in the blend, is observed in all curves regardless of the KGM content. The melting temperatures (T_m), heat increment (ΔC_p) and the enthalpies of fusion (ΔH_m) are shown in Table 2. It is observed that the T_m shifted gradually to a lower temperature and the width of the endothermic peak became broad with an increase of KGM content. This is due to that the incorporation of KGM into starch matrix decreases the inter-molecular force of starch, and partly decreases the crystallinity of ST, resulting in a decrease in the degree of crystallinity in the blends as KGM content increased as shown in the results from XRD. It is observed from Table 2 that ΔH_m of ST/KGM (from 90-10-15 to 0-100-15) is lower than that of 100-0-15, and the lowest ΔH_m occurred in the blend film with 50% KGM content. When the KGM content is higher than 50%, the ΔH_m of ST/KGM increased, but still lower than that of the neat ST. Generally, the retrogradation of ST is greatly dependent on the hydrogen bond-forming abilities of the additives with starch molecules. The stronger the hydrogen bond between starch and the additives, the more difficult for starch to re-crystallize during the storage period of ST (Cao, Chen, Chang, & Huneault, 2007). It demonstrated that the KGM formed relative strong hydrogen bonding between ST and KGM to suppress starch retrogradation. As a result, the values of ΔC_p and ΔH_m of the blends were lower than that of the neat PS film.

3.5. Mechanical properties

The results of mechanical properties for ST/KGM composites (from 100-0-15 to 0-100-15) are presented in Figs. 6 and 7. Both the tensile strength (σ_b) and elongation at break (ε_b) of the blends are remarkably higher than those of the neat starch (100-0-15). The stepwise increase of σ_b and σ_b increases with an increase of KGM content at the fixed glycerol content. Indeed, the mechanical properties of the blend films are affected by the glycerol content. With the increase of plasticizer concentration, the tensile strength decreased, and the elongation at break increased.

On the whole, the σ_b and ε_b of the films increased with an increase of KGM content in the blend films. When the KGM content is 70 wt%, the σ_b reached a maximum of 68.1 MPa in the film 30-70-10; and the ε_b reached a maximum of 59.0% in the film 30-70-15. All the σ_b and ε_b of the blend films are higher than that of the corresponding the neat starch films with the same glycerol content. This is due to the breakage of inter-molecular hydrogen bonding and formation of the intra-molecular interaction between ST and KGM. As reported in previous work, KGM facilitated to form synergistic interactions with individual carrageenan, xanthan, gellan, and corn starch (Yoshimura et al., 1998), and the synergistic interactions between KGM and ST in this case resulted in an improvement in both tensile strength and elongations at break of the ST/KGM blend films. On the other hand, the synergistic interaction can tend to improve the motion of the chain segments adjacent to it and impact re-crystallize in starch (Carvalho & Grosso, 2006). It has been reported that the special interactions between the amylose of starch and KGM molecules are stronger than that between amylopectin and KGM, thus it is easier for amylose than the branched chain amylopectin to blend with KGM (Avérous &

Table 2
The DSC data of starch/KGM blends when 15% glycerol were used: associated heat increment (ΔC_p), melting temperature (T_m), and associated heat of fusion (ΔH_m)

RH (%)	s-k-g	ΔC_p (J g^{-1} K^{-1})	T_m (°C)	ΔH_m (J g^{-1})
43	100-0-15	43.096	174.4	254.3
	90-10-15	39.395	170.4	203.5
	70-30-15	13.078	160.1	236.0
	50-50-15	1.708	129.9	69.5
	30-70-15	2.360	121.4	114.0
	10-90-15	4.520	117.4	211.9
	0-100-15	2.063	112.0	126.4

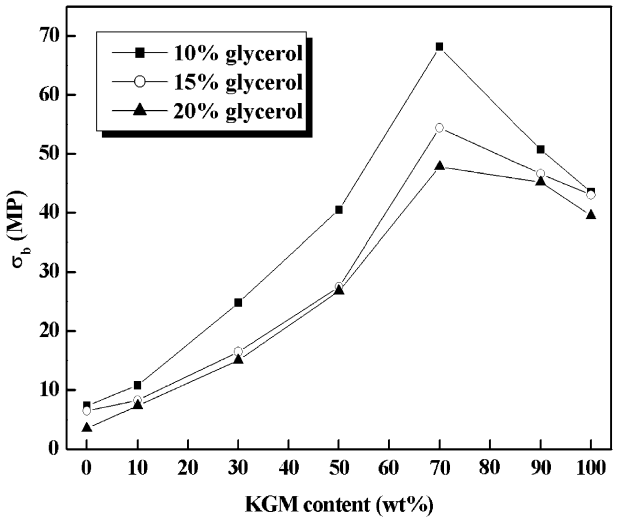

Fig. 6. Dependence of tensile strength of ST/KGM blend films on KGM content.

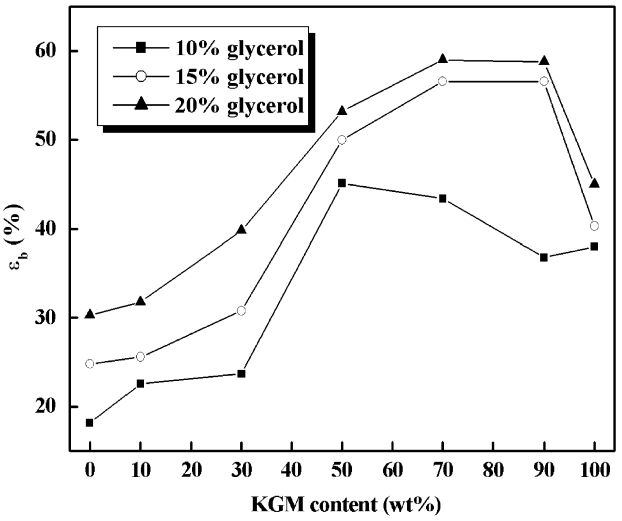

Fig. 7. Dependence of elongation at break of ST/KGM blend films on KGM content.

Boquillon, 2004; Cao et al. 2007). The amylose of starch is similar to the KGM in structure, which makes it compatible with KGM. Due to this reason, the tensile strength and elongation at break of the blend films were improved at the same time, which might lead to potential applications in biodegradable package.

3.6. Moisture uptake of the films

The moisture uptake at equilibrium of the blend films with different KGM content at 98% of *RH* are plotted in Fig. 8. It is observed that the neat starch (100-0-15) absorbed around 53.2 wt% of moisture. The moisture uptake at equilibrium increased as the KGM content increased. This is due to the higher water absorption tendency of KGM than ST. The KGM might facilitate the moisture permeation into starch when submitted to highly moisture atmospheres. In general, the increase of moisture uptake will decrease the tensile strength. However, in this work, with an increase of KGM content in the blend films, both the moisture uptake and tensile strength of the films simultaneously increased. This indicates that the blend films exhibit higher tensile strength in addition to the greater moisture retention than that of the neat starch film, which might offer interesting and valuable properties to the composites as edible films and coatings.

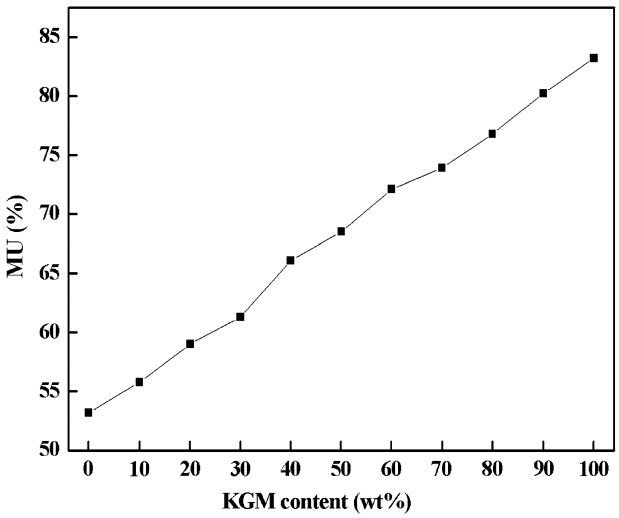

Fig. 8. Moisture uptake at equilibrium of ST/KGM blend films conditioned at atmosphere as a function of KGM content.

4. Conclusions

A series of composite films were prepared from glycerol-plasticized starch (ST) and konjac glucomannan (KGM). The results from FT-IR, XRD and SEM indicated that ST and KGM interacted and formed strong hydrogen bonding, resulted in good miscibility. With an increase of KGM content, the melting temperature of starch crystallinities decreased. Compared with the neat ST film (100-0-15), the tensile strength of the blend films increased from 7.4 to 68.1 MPa as KGM content increased from 0 to 70 wt% while 10 wt% of glycerol was used as a plasticizer. It is worth noting that the values of elongation at break of ST/KGM blend films were all higher than that of KGM film (0-100-15), and reached a maximum value of 59.0% when the content of KGM and glycerol was 70 wt% and 20 wt%, respectively. The presence of KGM also increased the moisture uptake of the blend films. The improvement of the properties of the ST/KGM maybe resulted from the formation of synergistic interaction and hydrogen bonding between KGM and ST molecules. The ST/KGM blends exhibited a potential application as edible food films and coatings.

Acknowledgement

This work was financially supported in part by Agricultural Bioproducts Innovation Program (ABIP) of Canada via the Pulse Research Network (PURENet).

References

Aburto, J., Alric, I., Thiebaud, S., Borredon, E., Bikiaris, D., & Prinos, J. (1999). Synthesis, characterization, and biodegradability of fatty-acid esters of amylose and starch. *Journal of Applied Polymer Science, 74*, 1440–1451.

Avérous, L., Fauconnier, N., Moro, L., & Fringant, C. (2000). Blends of thermoplastic starch and polyesteramide: Processing and properties. *Journal of Applied Polymer Science, 76*, 1117–1128.

Avérous, L., & Boquillon, N. (2004). Biocomposites based on plasticized starch: Thermal and mechanical behaviors. *Carbohydrate Polymers, 56*, 111–122.

Calverta, R. J., Tepperc, S., Kammounib, W., Anderson, L. M., & Kritchevsky, D. (2006). Elevated K-ras activity with cholestyramine and lovastatin, but not konjac mannan or niacin in lung – Importance of mouse strain. *Biochemical Pharmacology, 72*, 1749–1755.

Cao, X. D., Chen, Y., Chang, P. R., & Huneault, M. A. (2007). Preparation and properties of plasticized starch/multiwalled carbon nanotubes composites. *Journal of Applied Polymer Science, 106*, 1431–1437.

Carvalho, R. A., & Grosso, C. (2006). Edible películas producidas con gelatina y casein cross-linked con transglutaminasa. *Food Research International, 39*, 458–466.

Cheng, L. H., Karim, A. A., Norziah, M. H., & Seow, C. C. (2002). Modification of the microstructural and physical properties of konjac glucomannan-based films by alkali and sodium carboxymethyl cellulose. *Food Research International, 35*, 829–836.

Chen, L. G., Liu, Z. L., & Zhuo, R. X. (2005). Synthesis and properties of degradable hydrogels of konjac glucomannan grafted acrylic acid for colon-specific drug delivery. *Polymer, 46*, 6274–6281.

Chillo, S., Flores, S., Mastromatteo, M., Conte, A., Gerschenson, L., & Del Nobile, M. A. (2008). Influence of glycerol and chitosan on tapioca starch-based edible film properties. *Journal of Food Engineering, 88*, 159–168.

Córdoba, A., Cuéllar, N., González, M., & Medina, J. (2008). The plasticizing effect of alginate on the thermoplastic starch/glycerin blends. *Carbohydrate Polymers, 73*, 409–416.

Fang, J. M., Fowler, P. A., Tomkinson, J., & Hill, C. A. S. (2002a). The preparation and characterization of a series of chemically modified potato starches. *Carbohydrate Polymers, 47*, 245–252.

Fang, J. M., Fowler, P. A., Tomkinson, J., & Hill, C. A. S. (2002b). An investigation of the use of recovered vegetable oil for the preparation of starch thermoplastics. *Carbohydrate Polymers, 50*, 429–434.

Fringant, C., Rinaudo, M., Foray, M. F., & Bardet, M. (1998). Preparation of mixed esters of starch or use of an external plasticizer: Two different ways to change the properties of starch acetate films. *Carbohydrate Polymers, 35*(1–2), 97–106.

García, M. A., Martino, M. N., & Zaritzky, N. E. (1998a). Starch-based coatings: Effect on refrigerated strawberry (Fragaria ananassa) quality. *Journal of the Science of Food and Agriculture, 76*, 411–420.

García, M. A., Martino, M. N., & Zaritzky, N. E. (1998b). Plasticized starch-based coatings to improve strawberry (fragaria × ananassa) quality and stability. *Journal of Agricultural and Food Chemistry, 46*, 3758–3763.

García, M. A., Martino, M. N., Zaritzky, N. E., & Plata, L. (2000). Microstructural characterization of plasticized starch-based films. *Starch – Stärke, 52*, 118–124.

Godbole, S., Gote, S., Latkar, M., & Chakrabarti, T. (2003). Preparation and characterization of biodegradable poly-3-hydroxybutyrate-starch blend films. *Bioresource Technology, 86*, 33–37.

Huang, M. F., & Yu, J. G. (2005). High performance biodegradable thermoplastic starch-EMMT nanoplastics. *Polymer, 46*, 3157–3162.

Ishiaku, U. S., Pang, K. W., Lee, W. S., & Mohd, I. Z. A. (2002). Mechanical properties and enzymic degradation of thermoplastic and granular sago starch filled poly(ε-caprolactone). *European Polymer Journal, 38*, 393–401.

Jagannath, J. H., Radhika, M., Nanjappa, C., Murali, H. S., & Bawa, A. S. (2006). Antimicrobial, mechanical, barrier, and thermal properties of starch-casein based, neem (melia azardirachta) extract containing film. *Journal of Applied Polymer Science, 101*, 3948–3954.

Jansson, A., Järnström, L., Rättö, P., & Thuvander, F. (2006). Physical and swelling properties of spray-dried powders made from starch and poly(vinyl alcohol). *Starch – Stärke, 58*, 632–641.

Krochta, J. M., & De Mulder-Johnston, C. (1997). Edible and biodegradable polymer films: Challenges and opportunities. *Food Technology, 51*, 61–77.

Liu, C. H., & Xiao, C. B. (2004). Characterization of konjac glucomannan-quaternized poly(4-vinyl-*N*-butyl) pyridine blend films and their preservation effect. *Journal of Applied Polymer Science, 93*, 1868–1875.

Ma, X. F., & Yu, J. G. (2004). The plasticizers containing amide groups for thermoplastic starch. *Carbohydrate Polymers, 57*, 197–203.

Martin, O., & Avérous, L. (2001). Plasticization and properties of biodegradable multiphase systems. *Polymer, 42*, 6209–6219.

Mathew, A. P., & Dufresne, A. (2002). Morphological investigation of nanocomposites from sorbitol plasticized starch and tunicin whiskers. *Biomacromolecules, 3*, 609–617.

Mathew, S. H., Brahmakumar, M., & Emilia Abraham, T. (2006). Microstructural imaging and characterization of the mechanical, chemical, thermal, and swelling properties of starch-chitosan blend films. *Biopolymers, 82*, 176–187.

Maurizio, A., Jan, J., & Vlieger, D. (2005). Biodegradable starch/clay nanocomposite films for food packaging applications. *Food Chemistry, 93*, 467–474.

Nakamura, E. M., Cordi, L., Almeida, G. S. G., Duran, N., & Mei, L. H. I. (2005). Study and development of LDPE/starch partially biodegradable compounds. *Journal of Materials Processing Technology*, 236–241.

Parandoosh, S., & Hudson, S. M. (1993). The acetylation and enzymatic degradation of starch films. *Journal of Applied Polymer Science, 48*, 787–791.

Patil, D. R., Fanta, G. F., Felker, F. C., & Salch, J. H. (2008). Application of hydrophilic starch-based coatings on polyethylene surfaces. *Journal of Applied Polymer Science, 108*, 2749–2755.

Pracella, M., Pazzagli, F., & Galeski, A. (2002). Reactive compatibilization and properties of recycled poly(ethylene terephthalate)/polyethylene blends. *Polymer Bulletin, 48*, 67–74.

Rindlav, A., Stading, M., Hermansson, A. M., & Gatenholm, P. (1998). Structure, mechanical and barrier properties of amylose and amylopectin films. *Carbohydrate Polymers, 36*, 217–224.

Sagar, A. D., & Merrill, E. W. (1995). Properties of fatty-acid esters of starch. *Journal of Applied Polymer Science, 58*, 1647–1656.

Seidenstücker, T., & Fritz, H. G. (1998). Innovative biodegradable materials based upon starch and thermoplastic poly(ester-urethane) (TPU). *Polymer Degradation and Stability, 59*, 279–285.

Singh, J., Kaur, L., & McCarthy, O. J. (2007). Factors influencing the physico-chemical, morphological, thermal and rheological properties of some chemically modified starches for food applications – A review. *Food Hydrocolloids, 21*, 1–22.

Szepes, A., Makai, Z., Blumer, C., Mader, K., Kása, P., Jr., & Szabó-Révész, P. (2008). Characterization and drug delivery behaviour of starch-based hydrogels prepared via isostatic ultrahigh pressure. *Carbohydrate Polymers, 72*, 571–578.

Walia, P. S., Lawton, J. W., Shogren, R. L., & Felker, F. C. (2000). Effect of moisture level on the morphology and melt flow behavior of thermoplastic starch/poly(hydroxy ester ether) blends. *Polymer, 41*, 8083–8093.

Walia, P. S., Lawton, J. W., & Shogren, R. L. (2002). Mechanical properties of thermoplastic starch/poly(hydroxy ester ether) blends: Effect of moisture during and after processing. *Journal of Applied Polymer Science, 84*, 121–131.

Wang, X. L., Yang, K. K., & Wang, Y. Z. (2004). Crystallization and morphology of a novel biodegradable polymer system: Poly(1,4-dioxan-2-one)/starch blends. *Acta Materialia, 52*, 4899–4905.

Wesslén, B. (1998). Amphiphilic graft copolymers – Preparation and interfacial properties. *Macromolecular Symposia, 130*, 403–410.

Wesslén, K. B., & Wesslén, B. (2002). Synthesis of amphiphilic amylose and starch derivatives. *Carbohydrate Polymers, 47*, 303–311.

Wolff, I. A., Olds, D. W., & Hilbert, G. E. (1951). Triesters of corn starch, amylose, and amylopectin. *Industrial & Engineering Chemistry Research, 43*, 911–928.

Yoshimura, M., Takaya, T., & Nishinari, K. (1998). Rheological studies on mixtures of corn starch and konjac-glucomannan. *Carbohydrate Polymers, 35*, 71–79.

Yu, L., Dean, K., & Li, L. (2006). Polymer blends and composites from renewable resources. *Progress in Polymer Science, 31*, 576–602.